Luminescence Properties of ZnO Nanocrystals and Ceramics

Larisa Grigorjeva, Donats Millers, Janis Grabis, Claude Monty, Aleksandr Kalinko, Krishjanis Smits, Vladimir Pankratov, and Witold Łojkowski

***Abstract*—The luminescence excitation spectra, luminescence spectra and the nanosecond-scale decay kinetics were studied. The ZnO and ZnO:Al nanopowders were prepared by vaporization-condensation in a solar furnace using different raw powders: commercial, hydrothermal and those obtained by plasma synthesis. Exciton-phonon as well as exciton-exciton interaction processes in nanopowders, a bulk crystal and ZnO ceramics were studied and compared. The fast decay and low afterglow intensity of ZnO nanopowders and ceramics support these materials for scintillators.**

***Index Terms*—Ceramic, fast luminescence, nanopowders, ZnO.**

I. INTRODUCTION

ZnO luminescence properties have been intensively studied recently due to progress in single crystal growth as well as preparation of nanostructured materials by hydrothermal, vapor condensation methods [1], [2], plasma synthesis [3] and other methods. Zinc oxide crystal is a well known direct band (3.37 eV) semiconductor with hexagonal wurtzite structure. Due to its unique luminescence parameters, ZnO is a promising material for different applications (for example, light-emitters (LED, displays) and thus the investigations of structural defects, excitonic processes and donor-acceptor centers are of high interest [1], [4], [5].

The density of ZnO is close to that of $(Y,Gd)_2O_3$:Eu,Pr ceramic used in a computed tomography (5.6 g/cm^3 and 5.9 g/cm^3, respectively). Large exciton binding energy (~60 meV) allows observation of the excitonic luminescence even at room temperature (RT). High radiation resistance allows the use of ZnO in radiation environments.

The time-resolved luminescence was studied in ZnO [5]–[9]. It is known that luminescence in the blue region is very fast (50 ps at 16 K [5]), therefore the ZnO is a promising material for fast scintillators. The main problem is to prepare high quality material and to enhance the luminescence yield. The vaporization-condensation (VC) technique leads to "whiskers" - type structures with low defect level [10], [11]. We did not find any studies of luminescence in ZnO ceramic, despite progress in the past few years in luminescent ceramic sintering. In this paper, we present the results of the time-resolved luminescence in ZnO nanostructured powders obtained by means of different techniques and compare the luminescence parameters of nanopowders, a single crystal and ceramic.

II. EXPERIMENTAL

A. Samples

Undoped and Al-doped nanopowders were obtained by plasma (PL) [1] and hydrothermal (HY) procedure and were characterized by SEM and BET methods. XRD results show presence of the only ZnO wurtzite structure for all samples under study.

on hydrolytic precipitation of ZnO using a water solution of zinc chloride $ZnCl_2$ and KOH as starting precursors, according to the reaction

$$ZnCl_2 + 2KOH \rightarrow Zn(OH)_2 + 2KCl. \qquad (1)$$

The obtained substance was filtered and repeatedly washed with distilled water, until KCl ions were removed. Then the powder obtained was dried at 90°C during 24 hours ($Zn(OH)_2 \rightarrow ZnO + H_2O$) and heated in the air to the temperature of 500°C at a rate of 1.5°C/min and subsequently annealed at 500°C for 1.5 h and cooled (freely) to room temperature. After the treatment, the powder was milled in a ceramic mortar. The ZnO:Al was obtained in similar way but the aluminium salt was added in appropriate amount to obtain the doped powder (see Table I).

PL powders consist of "wire"-like particles (Fig. 1) with the average size <1 μm length and $\sim$ 100 nm diameter. The HY method is based

Commercial (com) powder (Aldrich 99.99; $S_{\rm BET} = 3.9$ m^2/g) has ~300 nm average grain size with a large size distribution and hexagonal particles are well resolved in SEM images. Powders were prepared by the VC method in a solar reactor [2], [11] from PL powders (VC_PL), commercial powder (VC_com) or HY powders (VC_HY). These powders have tetrapods or "whisker" morphology (Fig. 2) with a diameter <50 nm; whisker length depends on a vaporization process conditions (air pressure in a reactor and solar power flow).

The ZnO:Al doped powders show as a rule smaller grains than undoped samples prepared by PL or VC methods under the same synthesis conditions.

Manuscript received June 26, 2007; revised February 13, 2008. This work was supported in part by DESY, HASYLAB, Contract RII3-CT-2004-506008 (IASFS), Latvian Material Science Project and EC6th FM Project SOLFACE. The work of K. Smits and V. Pankratov was supported by the ESF.

L. Grigorjeva, D. Millers, A. Kalinko, K. Smits, and V. Pankratov are with the Institute of Solid State Physics, University of Latvia, Riga LV-1063, Latvia (e-mail: lgrig@latnet.lv; dmillers@latnet.lv; akalin@latnet.lv; smits@cfi.lu.lv; vpank@latnet.lv).

J. Grabis is with the Institute of Inorganic Chemistry, Riga Technical University, Salaspils, Latvia (e-mail: grabis@nki.lv).

C. Monty is with CNRS Processes, Materials and Solar Energy Laboratory (PROMES), Odellio, Font Romeu 66120, France (e-mail: Claude.Monty@rpomes.cnrs.fr).

W. Łojkowski is with the Institute of High Pressure Physics, Polish Academy of Sciences (UNIPRESS), Poland (e-mail: wl@unipress.waw.pl).

Digital Object Identifier 10.1109/TNS.2008.921931

TABLE I
SAMPLES ABBREVIATIONS

Sample	Preparation method
PL	Plasma synthesis
HY	Hydrothermal synthesis
com	Commercial powder
VC_PL	Solar physical vapor deposition from PL powder
VC_HY	Solar physical vapor deposition from HY powder
VC_com	Solar physical vapor deposition from commercial powder

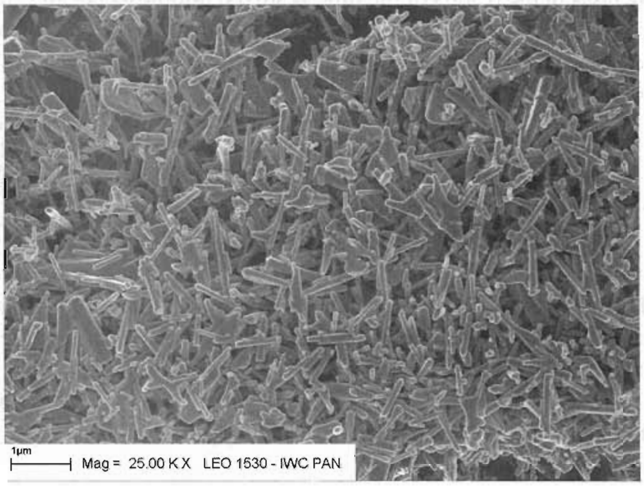

Fig. 1. SEM image of ZnO powder prepared by PL method.

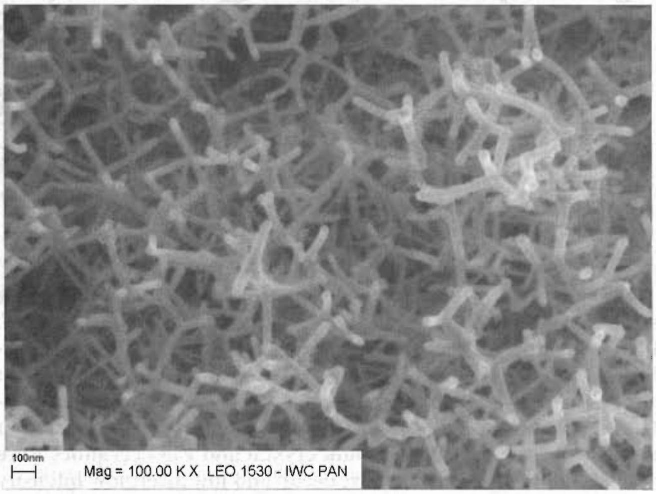

Fig. 2. SEM image of ZnO:Al powder prepared by VC_PL nanopowder.

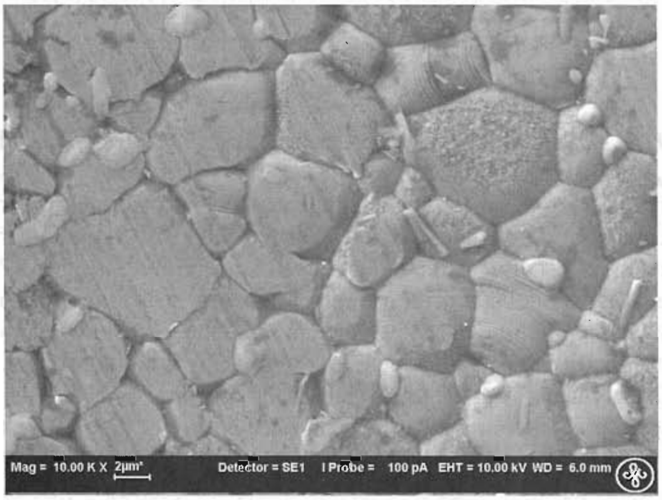

Fig. 3. SEM image of ZnO ceramic sintering from PL powder.

Average grain size (~50 nm) for PL sample was estimated from XRD and S_{BET} methods. A relatively wide distribution of particles has been observed using SEM and XRD for ZnO prepared by VC method.

ZnO ceramics were sintered from commercial and PL raw powders under different sintering conditions. For the ceramic prepared from com powder: 48 h at 1400°C in air, the average grain size was ~10–15 μm. The ceramic, sintering from PL powder: a powder was pressed under 1.0 MPa pressure and sintered in air for 2 h at 1150°C, the average grain size was ~3 μm (Fig. 3).

B. Luminescence Measurements

A pulsed YAG:Nd laser (266 nm, 10 ns pulse duration) was used for photoluminescence excitation. Luminescence measurements were carried out with a photon counting head (HAMAMATSU H8259) and photon counting board (fastComTec Communication Technology module P 7888-1E) with time resolution 2 ns.

The equipment for luminescence detection always had the same configuration. The comparison of luminescence relative intensities is possible since the all samples under study had the same size.

A pulsed (10 ns) electron beam was used for cathodoluminescence excitation. Electron fluence was 10^{12} el/cm^2, the electron energy ~ 270 keV. The output signal from a photomultiplier tube was displayed on a storage oscilloscope. The time resolution of the equipment was 15 ns.

The luminescence spectra, luminescence excitation spectra and luminescence decay kinetics were measured under VUV excitation using the SUPERLUMI setup in SR HASYLAB [12]. The synchrotron excitation pulses at HASYLAB are 130 ps fwhm and the time resolution of the registration system is ~1.0 ns.

III. RESULTS AND DISCUSSION

A. Low Temperature Luminescence Spectra

The low temperature luminescence spectra of a ZnO single crystal were measured under 10 eV excitation (Fig. 4). The observed peaks are similar to those in previous ZnO crystal studies. The origin was discussed [4] and these peaks are due to an exciton bound at a neutral donor (Ex,D°), its LO phonon replicas and two-electron satellite (TES) band. The TES is a radiative recombination of Ex,D°after the donor excitation. The energy

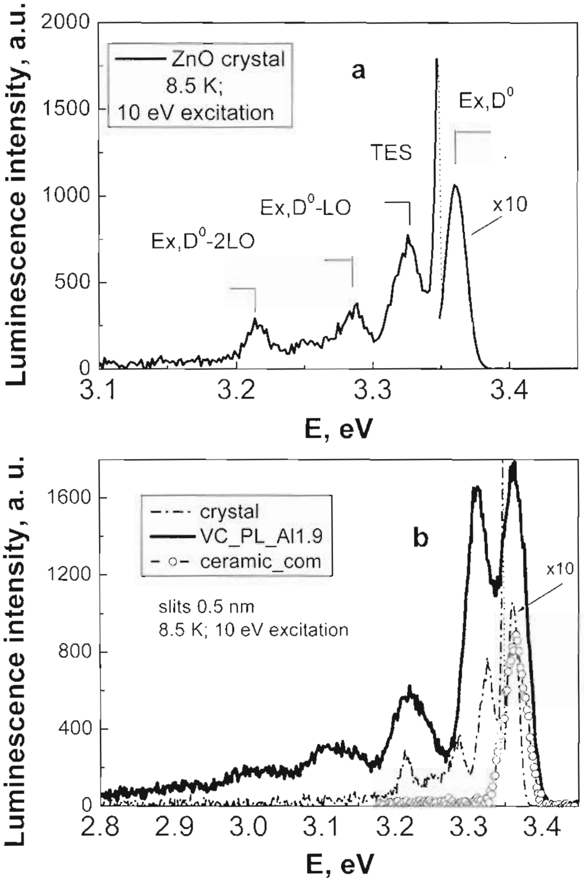

Fig. 4. Luminescence spectra of a ZnO single crystal (a), VC_PL ZnO:Al and ZnO ceramic (b); delay time 2 ns.

shift Ex,D°-TES is the energy difference between donor ground and excited states.

The spectra obtained for Al doped VC_PL nanopowder [see Fig. 4(b)] differ from those in a single crystal. The intensity of Ex,D° peak decreases and the TES band intensity is close to the Ex,D° peak intensity. Note that in a single crystal the exciton peak intensity was an order of magnitude higher that the TES band intensity. This means that the TES mechanism is effective in nanopowders. The bands due to exciton-phonon interaction are broader in nanopowders. In a ceramic sample the main band is the Ex,D°band, the TES and exciton-phonon replicas were not observed.

B. Excitation Spectra

The luminescence excitation spectra for the Ex,D° luminescence peak were measured at 8.5 K and the results obtained for a ZnO single crystal and ceramic are shown in Fig. 5. The spectra are normalized at 8.0 eV. The excitation spectra shapes are similar for a single crystal and ceramic (Fig. 5), as well as for nanopowders (not shown).

Hence, in all ZnO samples studied exciton creation under electron-hole pair excitation is effective in the 4.0–20 eV spectral range. In the spectral region >9 eV the effect of multiplication of electronic excitation was detected and it is known that it is important effect for scintillators.

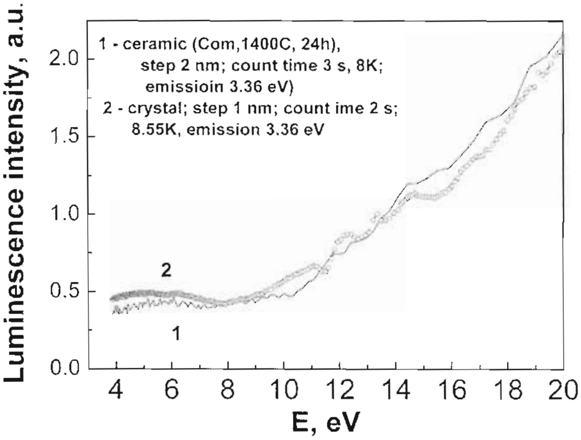

Fig. 5. Excitation spectra for 3.36 eV luminescence in ZnO single crystal and ceramic.

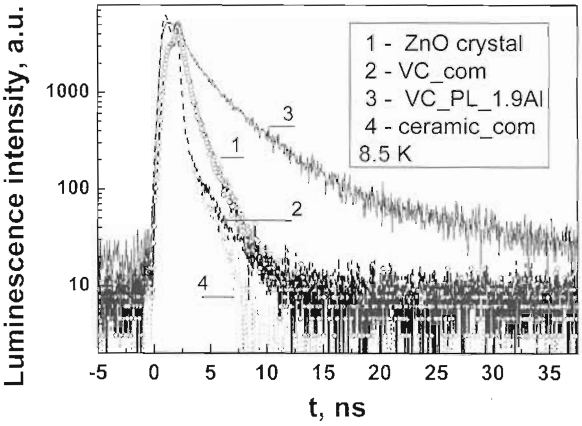

Fig. 6. Luminescence decay kinetics for 3.36 eV peak; 14 eV excitation.

C. Luminescence Decay Kinetics

In Fig. 6 the luminescence decay kinetics for the Ex,D_0 band is shown. The intensities are normalized at 2.5 ns. As stated above, the decay time of the excitonic luminescence is several nanoseconds and our experimental set-up has insufficient time resolution for correct decay time measurements. However, a comparison of decay processes in a single crystal, nanopowders and ceramics can be done. The decay times for the crystal, VC_com nanopowder and ceramic were fast and the excitation pulse duration determines the luminescence kinetics during first 2.5 ns. The results suggest that ZnO single crystals as well as nanopowders and ceramics could be used for fast scintillators.

A slower decay was measured for the 3.36 eV band in VC_PL ZnO:Al (see Fig. 6). In view of the fact that the Ex,D°and TES peaks overlap [see Fig. 4(b)], suggests that the TES is responsible for the slow decay contribution in decay kinetics.

D. Luminescence Spectra at RT

It is known that the luminescence spectra, luminescence yield and luminescence decay of nanocrystalline materials strongly depend on synthesis methods and surface conditions. A wide luminescence band peaking between 1.8–2.0 eV (yellow-red luminescence) was observed in HY samples [13]. In powders prepared by PL method as well as in powders prepared by the VC

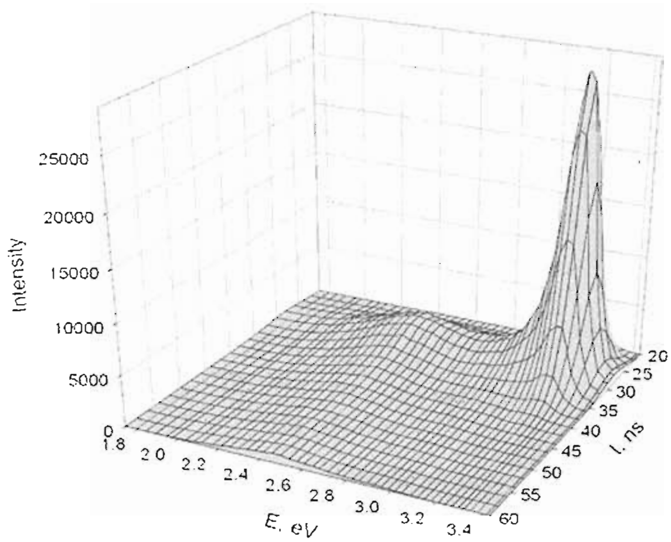

Fig. 7. Time-resolved luminescence spectra of VC_HY ZnO:Al (0.16 wt.%); YAG laser excitation (266 nm); RT.

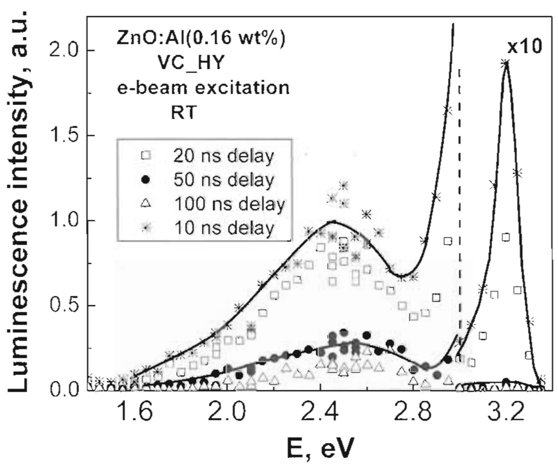

Fig. 8. Cathodoluminescence spectra measured after different delay times after excitation pulse starts of VC_HY ZnO:Al; RT.

process from HY target (VC_HY), a band peaking at ~2.4 eV (green luminescence) was detected. Variation of synthesis conditions results in spectra peak position shifts. We suggest that two types of defects are responsible for this luminescence and in some samples both bands have been detected. The three-dimensional (3D) plot of luminescence intensity versus time and photon energy for VC_HY ZnO:Al nanopowder is shown in Fig. 7.

Similar spectra were observed under electron beam excitation (Fig. 8).

The luminescence mechanism of the wide yellow-green emission line is recombination at defect states. Before VC process, the main luminescence band due to defects was detected at 2.0 eV; the intensity of the 3.26 eV band (due to annihilation of 1LO Ex at RT) was ~20 times weaker than for the VC sample. The surface defect is involved in a radiative recombination in HY powder. It is suggested that the whisker structures obtained in the VC process are more perfect nanocrystals than those obtained by the HY method [10], [11]. Excitonic luminescence intensity was enhanced in such structures. Hence, the VC process is very important for high quality ZnO nanopowder preparation.

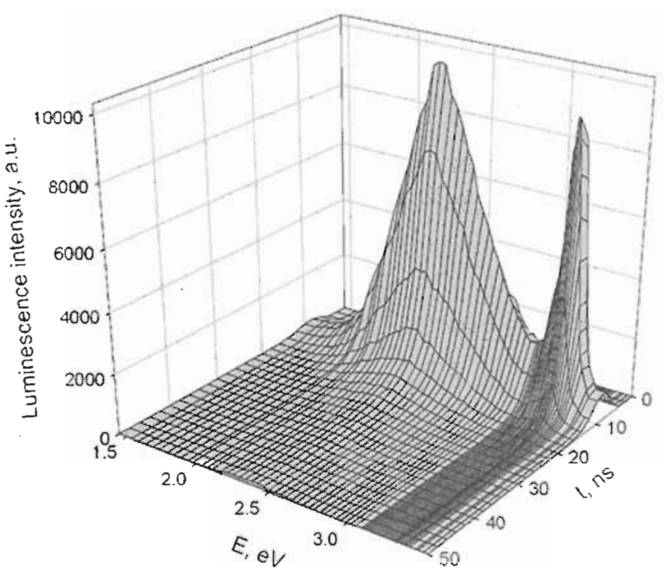

Fig. 9. Time-resolved luminescence spectra of ZnO ceramics sintering from powder obtained by plasma method; YAG laser excitation (266 nm), RT.

Time-resolved photoluminescence of ZnO ceramics at RT (Fig. 9) shows the luminescence bands at 2.2–2.4 eV and 3.26 eV known in ZnO single crystals and nanopowders. The luminescence spectra show that the same defect states occur in ceramics and raw powders, though the ceramic sintering temperature is high (> 1000°C). The decay kinetics in defect band was not exponential: a rough estimate shows that the luminescence intensity falls by an order of magnitude at first 150 ns in a single crystal, at 100 ns in nanopowders and at ~50 ns in ceramic. The afterglow level in a ceramic sample is quite low (<1% at 400 ns). Therefore, the decay time for the defect luminescence peak is significantly faster in ceramics than that in ZnO single crystals and ZnO raw powders.

We compare the luminescence kinetics obtained under the same experimental conditions for well known fast scintillator $PbWO_4$:La and ZnO ceramic (Fig. 10). The luminescence decay is faster for ZnO ceramic. The area under decay curve (S) is proportional to the light yield. We calculate the areas under decay kinetics for time range 0–45 ns and it is founding that $(S_{ZnO}/S_{PWO}) \cong 5$. It means that the light yield in fast component for ZnO is considerably higher than that for $PbWO_4$:La. We suggest that ZnO luminescence in blue spectral region is good tool for fast scintillator.

Summing up, the fast luminescence in the blue spectral region was observed in all ZnO ceramics studied. The exciton luminescence in sintered ceramic depends on the raw material used, sintering conditions and luminescence excitation density. The luminescence properties of ZnO ceramics make it promising for *fast* scintillator, especially if transparent ZnO ceramics could be sintered.

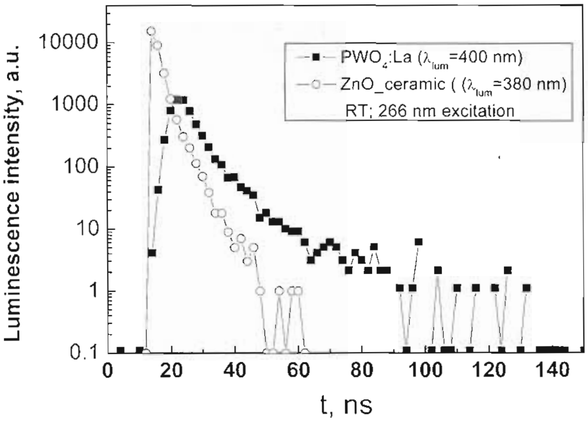

Fig. 10. Luminescence kinetics for ZnO ceramic and $PbWO_4$:La single crystal.

IV. CONCLUSION

The intensive TES luminescence observed in *nanocrystals* satisfy efficient exciton-donor interaction and energy transfer from exciton to donor.

The luminescence properties of a single crystal, nanopowders and ceramics, nanopowders were studied and compared. The two well separated luminescence peaks at 2.4 eV and 3.26 eV were observed in ZnO ceramics at room temperature. The peak at 2.4 eV was due to defects and the band at 3.26 eV due to excitons. The decay of both bands is fast in ceramics, particularly for the 3.26 eV emissions (<1 ns). The fast decaying luminescence shows that the ZnO ceramics is a promising material for a fast scintillator.

ACKNOWLEDGMENT

The authors thank T. Strachowski, J. Fidelus, and R. Piticesku for hydrothermal nanopowders preparations and discussions and A. Presz for SEM image measurements.

REFERENCES

[1] K. H. Tam *et al.*, "Defects in ZnO nanorods prepared by hydrotrhermal method," *J. Phys. Chem. B*, vol. 110, pp. 20865–20871, 2006.

[2] R. P. Piticesku, R. M. Piticescu, and C. J. Monty, "Synthesis of Al-doped ZnO nanomaterials with controlled luminescence," *J. Eur. Ceramic Soc.*, vol. 26, pp. 2979–2983, 2006.

[3] J. Grabis, I. Šteins, D. Jankoviča, A. Dulmanis, and G. Heidemane, "Preparation of nanosized oxide-based powders by gas and liquid phase methods," *Latv. J. Phys. Techn. Sci*, vol. 36, pp. 36–43, 2006.

[4] Ü. Özgür *et al.*, "A comprehensive review of ZnO materials and devices," *J. Applied Phys.*, vol. 98, pp. 041301–042103, 2005.

[5] G. Xiong, K. B. Ucer, R. T. Williams, J. Lee, D. Bhattacharyya, J. Metson, and P. Evans, "Donor-acceptor pair luminescence of nitrogen-implanted ZnO single crystal," *J. Appl. Phys.*, vol. 97, pp. 043528-1–043528-4, 2005.

[6] D. Ehrentraut, H. Sato, Y. Kagamitani, A. Yoshikawa, T. Fukuda, J. Pejchal, K. Polak, M. Nikl, H. Odaka, K. Hatanak, and H. Fukumura, "Fabrication and luminescence properties of single-crystalline, homoepitaxial zinc oxide films doped with tri- and tetravalent cations," *J. Mater. Chem.*, vol. 16, pp. 3369–3374, 2006.

[7] A. van Dijken, E. A. Meulenkamp, D. Vanmaekelbergh, and A. Meijerink, "The kinetic of the radiative and nonradiative processes in nanocrystalline ZnO particles upon photoexcitation," *J. Phys. Chem. B*, vol. 104, pp. 1715–1723, 2000.

[8] S. E. Derenzo, M. J. Weber, and M. K. Klintenberg, "Temperature dependence of the fast, near-band-edge scintillation from CuI, HgI_2, ZnO:Ga and CdS:In," *Nucl. Instr. Meth. A*, vol. 486, pp. 241–219, 2002.

[9] P. J. Sinpson, R. Tjossem, A. W. Hunt, K. G. Lynn, and V. Munné, "Superfast timing performance from ZnO scintillators," *Nucl. Instr. Meth. A*, vol. 505, pp. 82–84, 2003.

[10] L. Grigorjeva, D. Millers, K. Smits, C. Monty, J. Kouam, and L. El Mir, "The luminescence properties of ZnO:Al nanopowderts obtained by solgel, plasma and vaporization-condensation methods," *Solid State Phenomena*, vol. 128, pp. 135–140, 2007.

[11] T. Ait-Ahcene, C. Monty, J. Kouam, A. Thorel, G. Petot-Ervas, and A. Djemel, "Preparation by solar physical vapor deposition (SPVD) and nanostructural study of pure and Bi doped ZnO nanopowders," *J. Eur. Ceramic Society*, vol. 27, pp. 3413–3424, 2007.

[12] G. Zimmerer, "SUPERLUMI: A unique setup for luminescence spectroscopy with synchrotron radiation," *Radiation Meas.*, vol. 42, pp. 859–864, 2007.

[13] D. Millers, L. Grigorjeva, W. Łojkowski, and T. Strachowski, "Luminescence of ZnO nanopowders," *Radiation Meas.*, vol. 38, pp. 589–591, 2004.